CHAPTER-1

General Introduction and Literature Survey

1.1. Energy: Global Trends and Policy Perspectives

The world's energy landscape is changing dramatically as countries strive to strike a balance between environmental sustainability, energy security, and economic progress. Fossil fuels, such as coal and oil, have been the world's largest energy reserve since the dawn of the industrial period, and the energy they provide has caused a sharp rise in atmospheric CO_2 concentrations [1]. One of these conditions arises as a result of the rapidly increasing energy demand brought on by population growth. Since it is very easy to produce energy from fossil fuels, more than 80 % of energy consumption to date has come from these sources. The world's scattered oil supplies, of which two-thirds are in the Middle East, pose a serious threat to the usage of fossil fuels and lead to economic dependence on other nations. In addition, the planet may warm by up to 4 °C if the emission rate stays constant [2]. Global energy consumption is predicted to increase by about 50 % by 2050, mostly due to population growth and economic expansion in emerging nations, according to the EIA's (Energy Information Administration) International Energy Outlook 2023. Although they presently make up over 77 % of the world's energy consumption, fossil fuels are expected to lose ground as countries move toward greener energy sources.

Over the past century, a lot of studies have been done on green energy and the quest for substitutes for traditional energy sources. The energy crisis appears to be imminent due to the population's exponential increase and the depletion of traditional energy sources, including coal, natural gas, and oil. Furthermore, the detrimental effects of greenhouse gases (GHGs) generated by the extensive burning of fossil fuels on the environment have also grown to be a significant worry [3–6]. Inexplicable climatic changes have been made possible by the sharp

rise in GHGs, which has been causing global warming [7,8]. To lessen the effects of climate change, the IPCC sixth assessment report (AR6, 2023) highlights how urgent it is to significantly reduce GHG emissions. The research emphasizes that significant cuts in the use of coal, oil, and natural gas are necessary for the energy sector to rapidly decarbonize to keep global warming to 1.5 °C over pre-industrial levels (IPCC, 2023). The yearly worldwide energy consumption from fossil fuel sources, as well as CO_2 emissions from the fossil, chemical, and manufacturing industries, for the past 20 years, are shown in **Figure 1.1**. According to BP's (British Petroleum) "Statistical Review of World Energy 2024," which provided a thorough analysis of the supply and demand for the main energy sources at the national level, fossil fuels continue to account for 74 % of the world's energy needs [9]. At the same time, a significant quantity of CO_2 emissions is unavoidable due to the widespread use of fossil fuels.

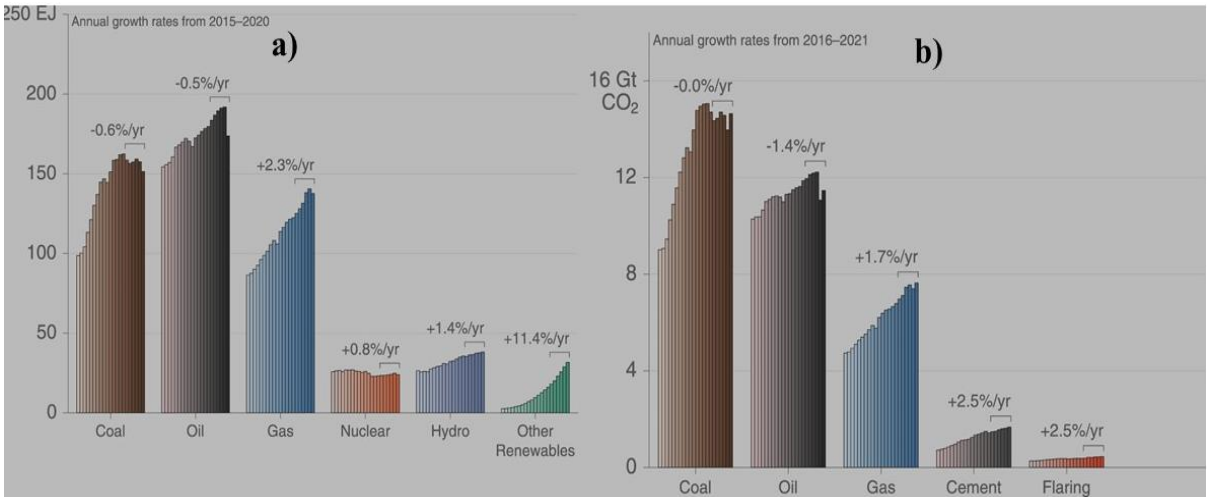

Figure 1.1. (a) Annual global energy consumption, **(b)** fossil CO_2 emission by fuel type (Coal oil and natural gas) and from cement production and flaring. (Global fossil carbon emissions rebound near pre-COVID-19 levels) (Reproduced with permission with reference to [10]).

About 10 % of all energy is produced using the more well-known and proven technologies of nuclear energy and hydroelectricity. Other sources of renewable energy, such as wind and solar, account for less than 5 % of the energy consumed overall. Many traditional energy sources, mostly fossil fuels, have dominated the market and are widespread. Fossil fuel usage has also been projected to reach around 3.3 terawatts by 2030, and it is anticipated to rise even more with the same forecast for coal, natural gas, and oil. To compete with fossil fuels, any future renewable technology must be developed to the terawatt level [11].

Energy must be effectively transformed, stored, and then made accessible when needed in order to address these issues. Establishing zero-emissions systems that run on wind, hydrogen, and oxygen and produce environmentally favorable by-products like water is a viable option in this regard. Water electrolyzers [12], fuel cells [13], metal-air rechargeable batteries [14], and other advanced sustainable technologies have all been thoroughly studied to meet the energy needs of many applications in the future, including stationary devices and vehicles [15]. They are also reasonably priced, environmentally beneficial, and theoretically have a high specific energy density. The hydrogen evolution reaction (HER) and the oxygen evolution reaction (OER) for energy conversion via electrocatalytic water splitting, the hydrogen oxidation reaction (HOR) and oxygen reduction reaction (ORR) in fuel cells, and both ORR and OER in rechargeable metal-air batteries are examples of the electrochemical reactions that are typically used in these systems. Therefore, the process that controls the overall functionality and advancement of these technologies, is OER [16–18]. Thus, the primary goal of this thesis is to efficiently generate molecular oxygen (O_2) by oxidizing hydroxide ions (OH^-), based on non-noble metals by overcoming a number of obstacles

including their high cost and insufficient stability, which will advance the technologies under discussion.

1.2. Comprehensive Overview of Sustainable Technologies

In order to create a robust future, sustainable technologies are essential. Societies may shift to a more sustainable and ecologically conscious lifestyle by investing in waste reduction techniques, eco-friendly infrastructure, renewable energy, and green mobility. The majority of researchers are interested in fuel cells, metal-air batteries, and water splitting among other renewable energy-based technologies because of their wide range of potential uses. Progress towards a cleaner, greener Earth will be fueled by ongoing research and innovation in these fields.

1.2.1. Fuel Cells

Fuel cells are electrochemical devices that use a reaction with oxygen to transform chemical energy from hydrogen or other fuels into electrical power. Fuel cells use an electrochemical method instead of fossil fuels to generate carbon-neutral electricity [19,20]. They are an ecologically benign energy source because of their high efficiency, which generates electricity with the waste of heat and water. The three primary parts of a fuel cell are an electrolyte, a cathode, and an anode. Hydrogen molecules divide into protons and electrons at the anode. While the electrons go via an external circuit to produce an electric current, the protons move through the electrolyte. Water is produced at the cathode when oxygen combines with protons and electrons.

The basic design of a fuel cell is comparable to that of a battery, with an electrolyte-containing permeable membrane between the anode and cathode electrodes. The essential concept is that the anode receives continuous gaseous fuel, the cathode receives oxygen from the atmosphere, and ions are exchanged across an electrolyte membrane to keep cells electroneutral. However, as long as fuel and oxidants are continuously available, they don't require recharging like batteries. Typical examples include solid oxide fuel cells (SOFCs), direct methanol fuel cells (DMFCs), alkaline fuel cells (AFCs), phosphoric acid fuel cells (PAFCs), proton exchange membrane fuel cells (PEMFCs), and others. The fuel cell classifications according to their operating conditions are provided in the following **Table 1.1**.

Table 1.1. Classification of Fuel Cells and their operating parameters.

Fuel Cell	Operating Temperature (°C)	Electrolyte	Migrating ion	Startup time
PEMFCs	~ 80	Acidic polymer electrolyte membrane	H^+	Fast
SOFCs	~ 1000	Hard ceramic compounds	O_2^-	Slow
AFCs	150-200	Potassium hydroxide	OH^-	Fast
MCFCs	~ 650	Sodium and magnesium carbonates	CO_3^{2-}	Slow
PAFCs	150-200	Phosphoric acid	H^+	Moderate
DMFCs	60	Nafion perfluorosulfonic acid	H^+	Fast

1.2.1.1. Proton Exchange Membrane Fuel Cells (PEMFCs)

Proton Exchange Membrane Fuel Cell (PEMFCs) is a type of fuel cell that generates electricity through the electrochemical reaction of hydrogen and oxygen, with water as the only byproduct. To produce electricity, it employs a solid polymer electrolyte membrane that lets protons flow through while obstructing electrons, requiring them to go via an external circuit. Because PEMFCs run at low temperatures (usually between 60 and 80 °C), they may be started quickly and are suitable for a range of uses, such as fixed power production, portable power, and transportation. Their small design, minimal emissions, and great power density are among their benefits. However, obstacles to general implementation still exist, including the requirement for high-purity hydrogen, impurity sensitivity, and the expense of platinum catalysts. PEMFCs are becoming an important component of the shift to clean energy as a result of ongoing improvements in design and materials that increase their efficacy, longevity, and affordability [21].

1.2.1.2. Solid Oxide Fuel Cells (SOFCs)

Solid Oxide Fuel Cells (SOFCs) are high-temperature, high-efficiency electrochemical devices using a solid ceramic electrolyte to transform chemical energy into electrical energy. They can use a range of fuels, such as hydrogen, natural gas, and biogas, and operate at temperatures between 600 and 1000 °C, making them incredibly adaptable. High efficiency (up to 60 % in standalone mode and over 85 % in combined heat and power applications), fuel flexibility, and minimal emissions since they don't require combustion are just a few benefits of SOFCs. Although its solid-state design guarantees longevity and endurance, high operating

temperatures pose problems with material deterioration and starting time. In spite of these challenges, research is still being done to improve performance and reduce operating temperatures, which makes SOFCs a viable option for environmentally friendly energy production in both fixed and mobile applications [22].

1.2.1.3. Alkaline Fuel Cells (AFCs)

An alkaline electrolyte, usually potassium hydroxide (KOH), is used in alkaline fuel cells (AFCs) to promote the electrochemical interaction between hydrogen and oxygen, which generates heat, water, and electricity. AFCs have been extensively utilized in space applications, including the Apollo and space shuttle missions, due to their high efficiency (up to 70 %) and quick starting times. Because they function at comparatively low temperatures (usually between 60 and 90 °C), they enable small and light designs. Pure hydrogen and oxygen are necessary for AFCs to function at their best since they are extremely sensitive to carbon dioxide (CO_2), which can react with the electrolyte and impair performance. Notwithstanding this drawback, research is still being done to increase CO_2 tolerance and lower prices, which might make AFCs a viable option for a range of terrestrial uses, such as military and backup power [23].

1.2.1.4. Molten Carbonate Fuel Cells (MCFCs)

High-temperature fuel cells known as Molten Carbonate Fuel Cells (MCFCs) employ a combination of molten carbonate salts as the electrolyte and run at temperatures between 600 and 700 °C. With great efficiency (up to 60 % in standalone mode and over 80 % in combined heat and power systems) and fuel flexibility (they can run on hydrogen, natural gas, biogas,

and even coal-derived fuels), they are primarily made for large-scale stationary power production. Since internal reforming is made possible by the high working temperature, MCFCs may convert hydrocarbons into hydrogen without the need for an external reformer, unlike certain other fuel cells. They are appealing for carbon capture applications as they can also absorb and use carbon dioxide. In contrast to fuel cells that operate at lower temperatures, their high-temperature operation results in material degradation and a shorter lifespan. In industrial and utility-scale applications, MCFCs continue to be a promising technology for effective, low-emission energy generation in spite of these obstacles [24].

1.2.1.5. Phosphoric Acid Fuel Cells (PAFCs)

Fuel cells known as Phosphoric Acid Fuel Cells (PAFCs) can function at moderate temperatures of between 150 and 200 °C since they employ liquid phosphoric acid as the electrolyte. Because of their dependability, robustness, and capacity to employ impure hydrogen fuel, they are mostly utilized in stationary power production and some transportation applications. By using waste heat, PAFCs may achieve over 85 % efficiency in combined heat and power (CHP) applications, while offering electrical efficiencies of over 40 %. Compared to alkaline fuel cells (AFCs), they are less sensitive to carbon dioxide, which increases their versatility regarding fuel sources. However, PAFCs are less suited for mobile applications because of their lower power density when compared to PEMFCs and their requirement for platinum catalysts, which raises expenses. In spite of these challenges, PAFCs have been effectively implemented for dependable and effective power generation in hotels, hospitals, and other commercial facilities [24].

1.2.1.6. Direct Methanol Fuel Cells (DMFCs)

Liquid methanol is used as a direct fuel source in Direct Methanol Fuel Cells (DMFCs), a kind of Proton Exchange Membrane Fuel Cell (PEMFC), which does not require external fuel reforming. While electrons produce electricity via an external circuit, they function at relatively low temperatures (usually between 50 and 120 °C) and employ a polymer electrolyte membrane to assist proton transfer. Because of their high energy density, ease of transport and storage of fuel, and straightforward system design, DMFCs are perfect for small-scale power production, military applications, and portable electronics. The expense of platinum catalysts, sluggish reaction kinetics, and methanol crossover, a phenomenon in which methanol enters the membrane and reduces efficiency, hinder broad deployment. To increase the viability of DMFCs as a clean and efficient energy solution, research is being done to improve membrane materials, catalyst efficiency, and overall performance [25].

1.2.2. Metal Air Batteries

Metal-air batteries are an energy storage technology that is less expensive, has a longer shelf life, and has a higher theoretical energy density (1084 Wh Kg^{-1}) than fuel cells [26]. With a metal anode, an electrolyte, and a porous air cathode that allows for oxygen uptake from the surroundings, metal-air batteries have a special structure. Typically, the anode is composed of metals that oxidize during discharge, such as iron, zinc, aluminum, or lithium. In order to facilitate ion movement between the electrodes, the electrolyte might be either aqueous or non-aqueous. One important part is the air cathode, which is made up of a porous, conductive substance (like metal oxides or carbon) covered with catalysts (such compounds based on

cobalt, manganese, or platinum) to improve the oxygen reduction process (ORR). The cathode's gas-diffusion layer facilitates effective oxygen uptake while halting electrolyte evaporation and gas contamination from outside sources. Additionally, some designs have a separator to lower the possibility of a short circuit by preventing direct contact between the anode and cathode.

Metal-air batteries are extremely energy-dense due to their lightweight design and air-breathing cathode; nonetheless, their broad commercialization requires addressing issues including electrode deterioration, restricted rechargeability, and electrolyte stability. There are two types of cell systems, depending on the type of electrolyte. Aqueous electrolyte is used in moisture-insensitive cell systems, while organic or aprotic solvents are used in moisture-sensitive cell systems. Batteries are primarily divided into two categories based on their operational principles: rechargeable and non-rechargeable as illustrated in **Figure 1.2**.

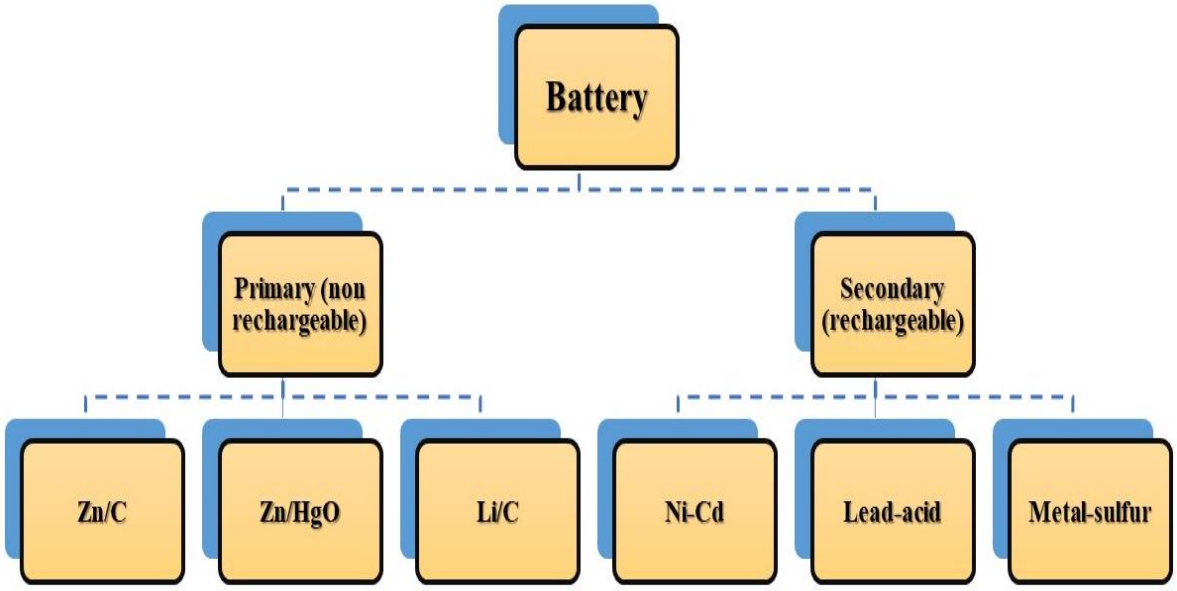

Figure 1.2. Flowchart illustrating the types of primary and secondary batteries.

Primary batteries are often single-cell, inexpensive, portable, and found in many home devices, including watches, cameras, devices, and more. They cannot be renewed once depleted and are no longer useful. The most common form of the primary battery has a greater energy density than zinc/carbon (Zn/C) batteries, which were later upgraded to Zn/alkaline MnO_2 batteries. Other major battery examples are Mg/MnO_2, Li/C, Zn/AgO_2, and Zn/HgO. Because of their high operational alkalinity and leakage issues, primary batteries can pose a serious environmental risk [27].

Conversely, secondary batteries are rechargeable and frequently found in devices like laptops, cell phones, and automobiles. Among the first inventions in this category are lead-acid batteries. They are commonly used in cars since they are typically inexpensive and have a high energy output. However, there is a continuous hunt for a new kind of secondary battery because of the toxicity of lead. The most advanced rechargeable storage technology available today for the majority of portable electrical and electronic devices is lithium-ion batteries (LIB). However, due to resource constraints, Na-ion batteries, Mg-ion batteries, and so forth were developed. Metal-air batteries are becoming a competitive alternative to metal-ion batteries due to their promising energy densities.

Metals such as Ca, Al, Fe, Cd, and Zn have been utilized in aqueous cell systems, whereas Li, K, Na, and Mg are used as the anode in aprotic electrolytes. Zn was shown to be the most corrosion-resistant element in alkaline electrolytes, an ideal metal for systems of aqueous cells [28]. The charging and discharging process is how metal-air batteries work. The metal anode (M) undergoes oxidation throughout the discharging process, releasing electrons and metal ions (M^{n+}). The generated electrons go through an external circuit to the cathode,

where the air undergoes an oxygen reduction process (ORR) to generate hydroxyl ions (OH^-) (**Equation 1.1**). After passing through the separator and electrolyte, these hydroxyl ions react to form $Zn(OH)_4^{2-}$ (**Equation 1.2**), which then breaks down to generate metal oxides (**Equation 1.3**). The oxygen evolution reaction (OER) occurs at the air electrode during the charging of air batteries, where oxygen is produced from water molecules and metal oxide at the anode reduced to solid metal.

$$O_2 + 2H_2O + 4e^- \leftrightarrow 4OH^- \qquad E= 0.40 \text{ V vs. SHE} \qquad \textbf{(1.1)}$$

$$Zn + 4OH^- \leftrightarrow Zn(OH)_4^{2-} + 2e^- \qquad E= 1.26 \text{ V vs. SHE} \qquad \textbf{(1.2)}$$

$$Zn(OH)_4^{2-} \leftrightarrow ZnO + H_2O + 2OH^- \qquad \textbf{(1.3)}$$

$$Zn + 2OH^- \leftrightarrow ZnO + H_2O + e^- \qquad E= 1.26 \text{ V vs. SHE} \qquad \textbf{(1.4)}$$

Superoxides or peroxides at the air electrodes are the discharge products. In this case, superoxides are formed from reduced oxygen molecules, which are then attached to metal ions. At the air electrode, the peroxide and superoxide produced during discharge are deposited and break down to oxygen molecules and metal ions during charging. **Equation 1.4** displays the zinc electrode's full reaction.

1.2.3. Water Splitting

Water splitting, a vital electrochemical process, uses an external energy source to separate water (H_2O) into oxygen (O_2) and hydrogen (H_2). The synthesis of hydrogen, a sustainable and clean energy source with uses in fuel cells, chemical synthesis, and energy storage, depends on this process. Several techniques, such as electrolysis (using electricity), photocatalysis (using light), and thermochemical or photoelectrochemical processes, can be used to split water. The

most common of these is electrolysis, in which water molecules are reduced at the cathode to make hydrogen and oxidized at the anode to produce oxygen [29].

1.2.3.1. Electrochemical Water Splitting

Catalysts are used in an electrochemical cell to lower the energy required for this process. Two redox half-cell processes make up water splitting: The hydrogen evolution reaction (HER) at the cathode, which forms H_2, and the oxygen evolution reaction (OER) at the anode, which produces O_2, as shown schematically in **Figure 1.3**. Due to the intricate multi-electron and proton transfer processes in the OER and HER, water electrolysis is naturally sluggish. To speed up these processes and increase total water splitting efficiency, robust catalysts must be improved. Although they are thought to be very powerful water splitting catalysts, noble metals like iridium, ruthenium, and platinum are not widely used due to their high cost and rarity.

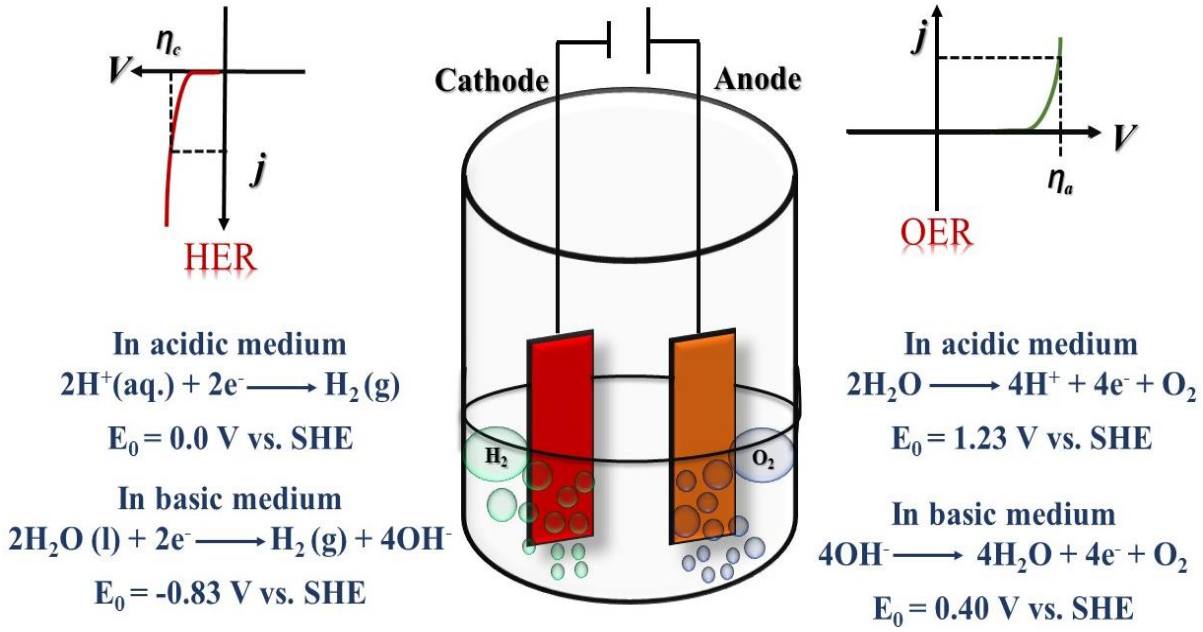

Figure 1.3. Pictorial representation of electrochemical water splitting.

In most cases, the electrolyte used in water splitting is either alkaline or acidic. HER is usually carried out in an acidic environment, whereas OER is frequently carried out in an alkaline environment. However, HER and OER must occur in the same electrolytic environment in order to achieve complete water splitting. Alkaline water electrolysis is frequently utilized, while water splitting may be done in both acidic and alkaline solutions. This choice stemmed from the possibility that acidic conditions may damage the membrane and the electrocatalyst, thus compromising the stability of the electrolysis system [28]. Alkaline water electrolyzers are already well-known and extensively available in the commercial sector due to their optimal working conditions. However, the alkaline HER must function effectively for alkaline electrolysis to be feasible, which is sometimes difficult because of its sluggish kinetics. As a result, increasing the reaction rate of alkaline HER remains a crucial focus for the advancement of alkaline water electrolysis technology. **Equation 1.5** provides the following representation of the total reaction involved in water splitting:

$$H_2O \longrightarrow H_2 + \frac{1}{2}O_2 \qquad \textbf{(1.5)}$$

1.3. Oxygen Evolution Reaction (OER)

The ability of electrical energy to split H_2O into H_2 and O_2 was one of the most inspirational scientific discoveries ever made in the 19th century, as proven by William Nicholson and Anthony Carlisle [30]. The OER that occurs at the anode of H_2O electrolyzers is currently unknown. However, it is still unknown exactly how the OER reaction works and what electrocatalysts are best for the reaction in terms of activity, stability, and durability [30]. In

energy conversion and storage devices, OER is an essential process, especially in regenerative fuel cells, metal air batteries, and water electrolysis. The reversal of oxygen reduction reaction (ORR), electrochemical OER, is technically an O-O bond production process at the anode that requires a $4e^-/H^+$ pair [31]. A multi-step technique is used to achieve the $4e^-$ total transfer required for an elementary OER process that is similar to ORR. The total efficiency of an energy-converting device is impacted by the slow kinetics of OER as a result [31]. Depending on the electrolyte's pH, the OER redox process may vary. In an acidic solution, two molecules of H_2O are converted to O_2 and $4H^+$, whereas OH^- ions are oxidized to O_2 and H_2O in an alkaline solution [32]. The anodic half-reactions at standard temperature and pressure (STP) in alkaline (**Equation 1.6**) as well as in acidic medium (**Equation 1.7**) can be represented by following equations.

In alkaline medium: $4OH^- \longrightarrow 2H_2O\,(l) + O_2\,(g) + 4e^-$; $E_a° = 0.404$ V vs. RHE **(1.6)**

In acidic medium: $2H_2O\,(l) \longrightarrow O_2\,(g) + 4H^+ + 4e^-$; $E_a° = 1.23$ V vs. RHE **(1.7)**

Although these processes appear straightforward, their slow kinetics and thermodynamics make them extremely challenging to conduct experimentally. The aforementioned OER reactions need a significant amount of energy since they involve four electrons in the generation of a single oxygen molecule, which includes the breaking of an O-H bond and the subsequent construction of an O-O bond [31,33,34].

1.3.1. Mechanism in OER

A deep comprehension of the chemical reactions taking place at the catalyst surface is necessary for the design of efficient OER electrocatalysts. Numerous possible methods have

been proposed. The three most widely accepted OER processes are the conventional adsorbate evolution mechanism (AEM), the lattice oxygen mechanism (LOM), and the oxide path mechanism (OPM). To better understand and guide the catalyst design, we compare these three processes in an alkaline medium [35].

1.3.1.1. The Adsorbate Evolution Mechanism (AEM)

The Adsorbate Evolution Mechanism (AEM) describes the stepwise oxidation of hydroxide or water molecules on a catalyst surface, leading to oxygen (O_2) formation (**Figure 1.4**). Hydroxide ions (OH^-) act as reactants, and the reaction progresses through surface-bound intermediates [36]. This mechanism is generally applicable to alkaline conditions. Under alkaline medium, the typical OER involving four electrons is (**Equation 1.8**):

$$4OH^- \rightarrow O_2 + 2H_2O + 4e^- \qquad \textbf{(1.8)}$$

Hydroxide ions from the electrolyte adsorb onto the active metal site (M), forming surface-bound hydroxyl species (**Equation 1.9**):

$$OH^- + M \rightarrow M{-}OH + e^- \qquad \textbf{(1.9)}$$

The adsorbed hydroxyl species (M−OH) undergo oxidation, leading to the formation of a metal-bound oxygen intermediate (**Equation 1.10**):

$$M{-}OH \rightarrow M{-}O + H^+ + e^- \qquad \textbf{(1.10)}$$

Another hydroxide ion binds to the oxygen intermediate, forming a peroxo-like species (M−OOH) (**Equation 1.11**):

$$M{-}O + OH^- \rightarrow M{-}OOH + e^- \qquad \textbf{(1.11)}$$

Finally, the peroxo intermediate dissociates, releasing molecular oxygen (O_2) and regenerating the metal active site (**Equation 1.12**):

$$M{-}OOH \rightarrow O_2 + M + H^+ + e^- \qquad \textbf{(1.12)}$$

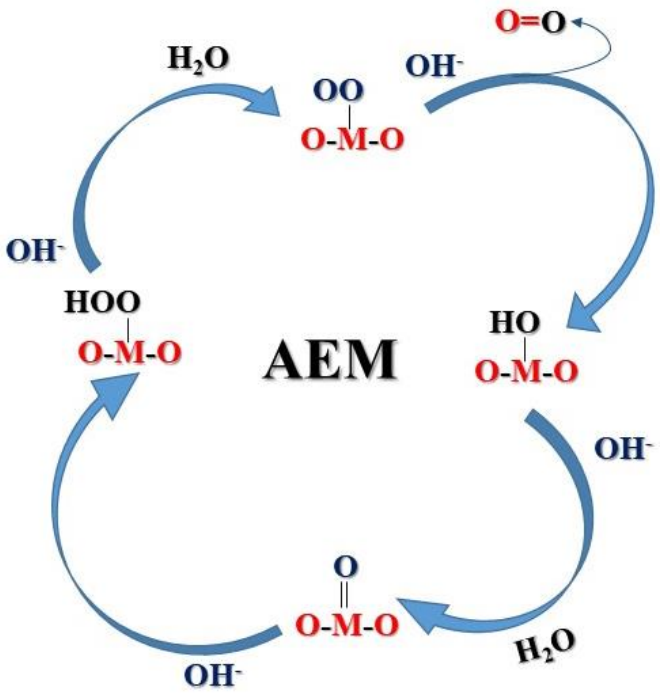

Figure 1.4. Plausible mechanism through AEM pathway.

1.3.1.2. The Lattice Oxygen Mechanism (LOM)

The Lattice Oxygen Mechanism (LOM) is an alternative pathway for the OER, distinct from the conventional AEM (**Figure 1.5**). In LOM, oxygen evolution occurs through the direct involvement of lattice oxygen atoms from the metal oxide catalyst, rather than solely relying on surface-adsorbed hydroxide species [37]. This process improves OER kinetics and lowers

energy barriers, making it especially important for perovskite oxides and catalysts based on transition metals. Under alkaline medium, the steps involved in a typical OER reaction involving four electrons can be written as follows:

The first step involves the hydroxide ions from the electrolyte interacting with the metal oxide catalyst (M-O) (**Equation 1.13**), leading to the hydroxylation of lattice oxygen.

$$OH^- + M{-}O \rightarrow M{-}OH + e^- \qquad (\mathbf{1.13})$$

In the next step, lattice oxygen (O_2) undergoes oxidation, creating an oxygen vacancy (V_O) and releasing protons and electrons (**Equation 1.14**):

$$M{-}OH \rightarrow M{-}O^+ + H^+ + e^- \qquad \mathbf{(1.14)}$$

In the subsequent step, neighboring lattice oxygen species couple to form an oxygen molecule (**Equation 1.15**):

$$2M{-}O^+ \rightarrow O_2 + 2M \qquad (\mathbf{1.15})$$

Finally, the oxygen vacancies are refilled by hydroxide ions from the electrolyte, restoring the catalyst structure (**Equation 1.16**):

$$2OH^- + 2M \rightarrow 2M{-}O + 2e^- \qquad \mathbf{(1.16)}$$

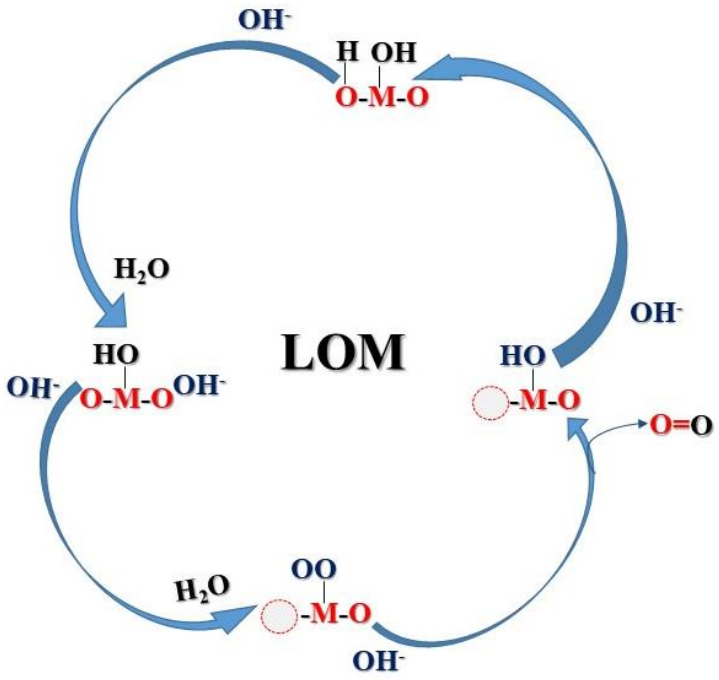

Figure 1.5. Plausible mechanism through LOM pathway.

1.3.1.3. The Oxide Pathway Mechanism (OPM)

OER activity and stability beyond theoretical limitations have been explained by an alternate oxide pathway mechanism (OPM) [38]. Direct O─O radical coupling is made possible by the OPM route without the need for further intermediates like HOO∗ or oxygen vacancies (**Figure 1.6**). Only O∗ and HO∗ species take part in this process as reaction intermediates. One of the main characteristics that sets the OPM apart is that strategically placed metal active sites cooperate to promote water dissociation and initiate O─O radical coupling without requiring the presence of lattice oxygen. As a result, the OPM route has stringent geometric restrictions on how metal active sites are arranged in space [39]. Under alkaline medium, the typical OER reaction involving four electrons is (**Equation 1.17**):

$$4OH^- \rightarrow O_2 + 2H_2O + 4e^- \quad \textbf{(1.17)}$$

In the first step, hydroxide ions adsorb onto the metal (M) catalyst surface (**Equation 1.18**), leading to the formation of metal hydroxide (M−OH):

$$OH^- + M \rightarrow M{-}OH + e^- \quad \textbf{(1.18)}$$

In the second step, the hydroxide undergoes further oxidation, forming a metal-oxyl ($M{-}O^-$) species (**Equation 1.19**):

$$M{-}OH \rightarrow M{-}O^- + H^+ + e^- \quad \textbf{(1.19)}$$

In the third step, the lattice oxygen species participate in oxygen evolution through O-O bond formation (**Equation 1.20**):

$$2M{-}O^- \rightarrow O_2 + 2M \quad \textbf{(1.20)}$$

Lastly, the active metal sites are restored as hydroxide ions from the electrolyte replenish the catalytic surface (**Equation 1.21**):

$$2OH^- + 2M \rightarrow 2M{-}OH + 2e^- \quad \textbf{(1.21)}$$

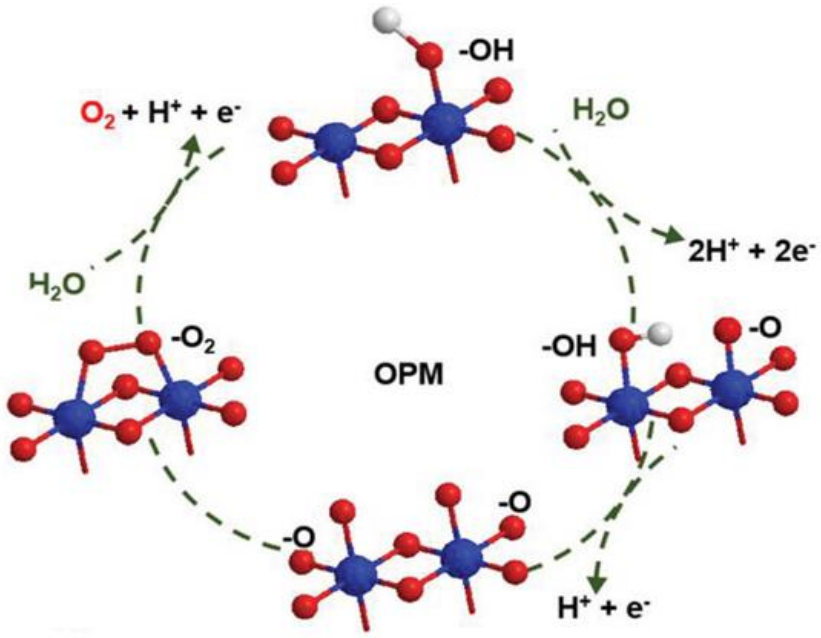

Figure 1.6. Schematic diagram of OPM pathway for OER [40].

1.4. Literature Review

The theoretical redox potential value of the OER is 1.23 V (vs. NHE) at STP in all electrolyte media [41]. Since OER is a relatively slow process, it requires a significant overpotential, which is a measure of potential greater than the theoretical thermodynamic potential to overcome the whole energy barrier [42]. OER activity is crucial for the effectiveness of FCs, MABs, and water splitting devices [43]. Consequently, breaking through the kinetic barriers and improving the overall energy-conversion efficiency depend on designing an OER electrocatalyst with increased activity. Since noble metals (such as Pt, Pd, Ru, Ir, and Rh) and later noble-metal oxides (such as IrO_2, RuO_2) were used as active electrocatalyst in both acidic and alkaline environments. Basic research on electrocatalysts for OER had begun in the 19th century [44,45]. The practical implementation of ECs is currently limited, nevertheless, due to

the low quantity and high price of these metals. For this reason, during the past 20 years, a lot of research has been done to find low-cost, high-activity, and sustainable ECs as substitutes [46].

OER is shown to be particularly active in transition metal oxides (TMOs) and other oxides, such as spinels, perovskites, and layered hydroxides (MOOH, $M(OH)_2$ $LiMO_2$, where M = Mn, Fe, Co, and Ni). Yoo *et al.* [47] demonstrated that the impact of participation on OER is performed by lattice oxygen in perovskites. Using density functional theory (DFT) calculations, they explained that OER through the lattice oxygen mechanism demonstrated superior activity compared to the conventionally employed adsorbate evolving mechanism. Ce modified-CuO_x produced by the electrodeposition approach with increased OER activity was recently reported by Chen *et al.* [48]. A simple manufacturing blueprint for Co_3O_4@CoO@Co nanoparticles (NPs) on graphene was published by Wu and colleagues [49] in 2020 in order to investigate their electrocatalytic potentials for OER in alkaline electrolytes. Karmakar *et al.* [50] created a one-step hydrothermal fabrication of graphite paper (GP) supported cobalt carbonate hydroxide ($Co_2(CO_3)(OH)_2$/GP) nanostructures and its Ni and Mn-substituted products, $Co_{1.9}Ni_{0.1}(CO_3)(OH)_2$/GP and $Co_{0.95}Mn_{0.05}CO_3$/GP, respectively, to investigate the impact of substitution in the crystal lattice. Notably, $Co_2(CO_3)(OH)_2$, replaced with Ni and Mn, showed noticeably improved OER performance in 1.0 M KOH. Similarly, to achieve efficient OER catalysis by electrochemical transformation, Wang and colleagues investigated Fe-doped cobalt carbonate hydroxide hydrate nanowires grown on nickel foam (referred to as Fe-CCHH/NF). With a modest Tafel slope of 50 mV dec^{-1} in 1 M KOH and an overpotential of

only 200 mV (vs. RHE) at a current density of 10 mA cm^{-2}, the Fe-CCHH/NF-30 exhibits superior OER catalytic activity [51].

Among the materials being studied, multimetallic compounds like $CaCu_3Ti_4O_{12}$ (CCTO), a typical $ACu_3Ti_4O_{12}$ (ACTO, where A = Sr, $Na_{1/2}Bi_{1/2}$ or $Na_{1/2}Y_{1/2}$, $Na_{1/2}La_{1/2}$, $Bi_{2/3}$, $Y_{2/3}$, $La_{2/3}$, Cd, Ca) have attracted attention due to their remarkable dielectric properties and thermal stability [52]. Despite being extensively studied for various applications, the potential of these materials for OER remains largely underexplored. $Bi_{2/3}Cu_3Ti_4O_{12}$ (BCTO), in particular, has emerged as a promising candidate for OER electrocatalysis due to its structural similarity to $CaCu_3Ti_4O_{12}$ (CCTO), a well-known perovskite-related oxide. However, the electrocatalytic properties of BCTO for OER are still in their early stages of investigation. Mg doping can enhance the intrinsic activity of BCTO by modifying its electronic structure, increasing conductivity, and promoting the availability of active sites, thereby improving its overall catalytic performance [53].

The OER in alkaline media has attracted much attention to tungsten-based oxides because of their low cost and chemical stability. Diverse tactics, including elemental doping, composite creation, and nanostructuring, have been used to enhance their catalytic activity. Nanostructured WO_3, such as nanowires and nanoarrays, improves OER kinetics by increasing surface area and charge transfer. An overpotential of 280 mV at 10 mA cm^{-2} in 1.0 M KOH was, for example, attained by WO_3 nanoarrays on carbon cloth [54]. Doping with transition metals like Co or Ni has been shown to tune the electronic structure and improve conductivity, with amorphous W-doped Co oxides showing an onset potential of ~230 mV and reaching 10 mA cm^{-2} at 320 mV overpotential [55]. Furthermore, by altering adsorption energies and

charge transfer properties, adding oxygen vacancies to WO_3 has been shown to increase catalytic activity [56]. Long-term water-splitting applications have also shown enhanced performance and durability with hybrid structures that combine tungsten oxides with carbon-based or semiconductor materials [57–59].

Synergistic effects and higher electron mobility have resulted in increased activity and stability for composite materials, which those combined with conductive polymers like polypyrrole [60–63]. The conducting polymer polypyrrole (ppy) has been extensively researched and has attracted a lot of interest as an electrocatalyst support material because of its superior electrical conductivity and ease of synthesis. Its conjugated π-electron system facilitates efficient electron transport, making it ideal for enhancing the electrochemical activity of metal-based catalysts [64]. Furthermore, the porous morphology of ppy facilitates ion diffusion and increases the electrochemically active surface area. For instance, α-MnSe/ppy composite has shown enhanced OER performance with reduced overpotentials and increased current densities. The ppy enhances the overall electrocatalytic activity, and overpotential is found to be 168 mV at 10 mA cm^{-2} current density [65].

When appropriately doped, ppy exhibits higher electrical conductivity than several other conducting polymers, such as polythiophene (PT) and polyaniline (PANI). Conductivity is crucial for OER because it permits efficient electron transfer between the electrode and the OER intermediates. In alkaline medium, polypyrrole is more stable than polythiophene and poly(3,4-ethylenedioxythiophene) (PEDOT) replacements, although many conducting polymers degrade under the harsh OER conditions, particularly in alkaline or acidic media. OER requires high working potentials, and because of its more stable electrochemical

structure, polypyrrole can withstand these conditions for longer than certain other conducting polymers. Other conducting polymers may oxidize or degrade structurally more quickly. Unlike other polymers with limited structural design flexibility (e.g., films, fibers, nanotubes), ppy may be synthesized in a range of morphologies. It is possible to increase overall catalytic effectiveness by adding more active sites for OER by modifying the surface area and porosity of these structures. These attributes highlight ppy's potential as a multifunctional support in advanced electrocatalyst design.

1.5. Key Parameters for Evaluating OER Activity

The following parameters are often used to assess and contrast different catalysts for water electrolysis. For effective electrocatalytic activity, our primary goal is to optimize the following parameters, which is briefly covered and summed up in **Figure 1.7**.

Figure 1.7. Parameters used to investigate electrocatalytic activity.

1.5.1. Onset Potential and Overpotential (η)

The additional voltage needed above and beyond the thermodynamic potential to drive the reaction at a noticeable rate is known as the overpotential (η) (**Equation 1.22**). The potential needed to split water into hydrogen and oxygen in an alkaline medium is 1.23 V vs. RHE (reversible hydrogen electrode). However, catalysts need a greater potential to overcome activation barriers because of sluggish kinetics. Several suitable catalysts can be used to reduce the overpotential for electrochemical process activation. Better electrocatalytic processes usually needed a lower overpotential value.

$$\eta\ (V) = E_{applied} - 1.23\ V\ (vs.\ RHE) \qquad \textbf{(1.22)}$$

The lowest voltage at which an electrochemical process, such as the OER, starts to proceed at a discernible pace is known as the onset potential. It is sometimes described as the potential at which a voltammogram shows a little but detectable current density (1 or 10 mA cm^{-2}, for example). For practical applications, the onset potential is often measured at a fixed current density of 10 mA cm^{-2}, which is a standard benchmark for evaluating OER catalysts [53,65,66]. Thus, the overpotential at 10 mA cm^{-2} (η_{10}) is a crucial parameter for assessing catalytic performance. A lower η_{10} value and a lower onset potential indicate a more efficient catalyst, as they reflect reduced energy requirements to drive OER.

1.5.2. Tafel slope (*b*)

The Tafel slope is an intrinsic property of a catalyst that provides insight into the reaction mechanism, the adsorption of intermediates, and the kinetics of an electrochemical process. It

is determined by plotting the overpotential as a function of the logarithm of the current density. Tafel slope can be expressed by the **Equation 1.23**.

$$d\log j/d\eta = 2.303RT/\alpha nF \qquad \textbf{(1.23)}$$

Where n is the number of electrons transferred, α is the charge transfer coefficient, T is the absolute temperature, R is the gas constant, j is the current density, η is the overpotential, and F is the Faraday's constant. Tafel slope is an important metric for assessing electrochemical performance since a lower value indicates better catalytic activity and quicker reaction kinetics. It helps researchers comprehend the underlying chemical pathways by offering important insight into the OER mechanism's rate-determining step (RDS) [67].

1.5.3. Electrochemically Active Surface Area (ECSA)

Another important metric for an electrocatalyst's intrinsic activity is electrochemically active surface area (ECSA). ECSA is the surface area of any electrocatalyst that tends to come into contact with the electrolyte for the purpose of transferring charges during an electrochemical reaction. Changing the electrolyte, material, and electrochemical process alters its value. For calculating ECSA, the double layer capacitance (C_{dl}) is measured from scan-dependent cyclic voltammetry (CV). Half of the slope from the plot of the charging current density vs. scan rate is then determined. The CV has been recorded inside a certain potential window of the non-faradaic potential range. Using **Equation 1.24**, the ECSA value is produced from dividing the C_{dl} value by the specific capacitance (C_s) [68]. Additionally, using the provided **Equation 1.25**, the electrocatalyst's roughness factor (R_f) was computed [69].

$$ECSA = \frac{C_{dl}}{C_s} \times S \qquad \textbf{(1.24)}$$

where S is the working electrode's geometrical surface area and C_s is its specific capacitance, which for a smooth surface is 40–60 μF cm^{-2} [70].

$$R_f = \frac{C_{dl}}{C_s} \qquad \textbf{(1.25)}$$

More active sites for the OER are indicated by a larger ECSA, which enhances catalytic activity. The intrinsic activity (specific activity) of a catalyst may be precisely assessed by normalizing the current density using ECSA, which helps to clarify its actual efficiency. ECSA is an important metric in the assessment of electrocatalysts since it also aids in determining whether improved catalytic performance results from the material's intrinsic qualities or just from an expanded surface area.

1.5.4. Reaction Order (p)

The reaction order (p) in an electrochemical system represents the dependence of the reaction rate on the concentration of a reactant, such as hydroxide ions (OH^-), in the OER (**Equation 1.26**). It helps in understanding the kinetics and mechanism of the reaction by indicating how changes in reactant concentration affect the overall rate, keeping the temperature and pressure constant.

$$p = \left(\frac{\partial \log i}{\partial \log[OH^-]}\right) \qquad \textbf{(1.26)}$$

It is crucial to conduct a series of current-potential (i-E) measurements at varying concentrations of the electroactive species while maintaining a constant temperature to

determine the reaction order in electrochemical systems. Plots of log j versus log [OH^-] at various fixed potentials across the catalyst/solution interface are created using these measurements. The gradients in these linear graphs illustrate the order of the reaction with the concentration of the species. The reaction order provides crucial insights into the rate-determining step (RDS), helping to unravel the reaction pathways and underlying mechanisms of an electrochemical process. It also serves as a valuable parameter for comparing different catalysts, enabling the assessment of their efficiency and performance in driving electrochemical reactions.

1.5.5. Standard Electrochemical Energy of Activation (E_a or $\Delta H_{el}^{0\neq}$)

The least amount of energy needed to initiate an electrochemical reaction is known as the electrochemical energy of activation ($\Delta H_{el}^{0\neq}$). For charge transfer and reaction kinetics to work effectively, it stands for the activation barrier that has to be broken. This parameter is essential for comprehending reaction pathways and maximizing catalyst performance in electrochemical systems. The energy of activation is often determined via Arrhenius equation by examining the temperature dependence of the reaction rate in an electrochemical process. Tafel polarization plots at different temperatures may be used to construct a plot of the log j vs. 1/T at a constant overpotential. Using the Arrhenius equation **(Equation 1.27)**, the activation energy (E_a or $\Delta H_{el}^{0\neq}$) is determined by the slope of this linear plot,

$$k = Ae^{-Ea/RT} \qquad \textbf{(1.27)}$$

Where, k is the rate constant,

A is the pre-exponential factor,

E_a is the activation energy,

R is universal gas constant (8.314×10^{-3} kJ $mol^{-1}K^{-1}$),

T is the absolute temperature.

In electrocatalysis, $\Delta H_{el}^{0\neq}$ is an important metric since a lower value indicates a more effective catalyst with quicker reaction kinetics. It helps to understand the energy needs for an electrochemical reaction by evaluating activation barriers, which offer important insights into reaction mechanism. By reducing activation energy through material design and electronic structure optimization, researchers aim to develop high-performance catalysts for energy conversion technologies.

1.5.6. Standard Electrochemical Enthalpy of Activation ($\Delta H^{0\neq}$)

The electrochemical enthalpy of activation ($\Delta H^{0\neq}$) represents the enthalpic energy barrier that must be overcome for an electrochemical reaction to proceed. It is a key thermodynamic parameter that provides insights into the energy requirements of charge transfer and reaction kinetics in electrocatalysis. For electrochemical processes, the standard enthalpy of activation ($\Delta H^{0\neq}$) is a widely used application of the transition state theory (TST) (**Equation 1.28**).

$$\Delta H_{el}^{0\neq} = \Delta H^{0\neq} - \alpha F \eta \qquad \textbf{(1.28)}$$

Where, $\Delta H_{el}^{0\neq}$ is the standard electrochemical energy of activation,

$\Delta H^{0\neq}$ is the standard enthalpy of activation,

α is the transfer coefficient,

F is faraday constant (96.5 kJ mol^{-1}),

η is the overpotential (at which activation energy is calculated),

For the calculation of the transfer coefficient, the following **Equation 1.29** could be used.

$$\alpha = 2.303RT/bF \qquad \textbf{(1.29)}$$

The above equation is used to compute the transfer coefficient value at various temperatures. The average value is then used to get the standard enthalpy of activation, $\Delta H^{0\neq}$. With a smaller $\Delta H^{0\neq}$, the energy barrier is lowered, improving catalyst efficiency and accelerating reaction kinetics. This characteristic is essential for evaluating various electrocatalysts and is important for choosing appropriate materials for metal-air batteries, fuel cells, and water splitting, among other uses.

1.5.7. Standard Electrochemical Entropy of Activation ($\Delta S^{0\neq}$)

The standard electrochemical entropy of activation ($\Delta S^{0\neq}$) represents the change in entropy associated with the transition state formation in an electrochemical reaction. It provides insights into the degree of order or disorder during the reaction process and helps in understanding the reaction pathway and mechanism. A positive $\Delta S^{0\neq}$ suggests increased disorder in the transition state, whereas a negative $\Delta S^{0\neq}$ indicates a more ordered transition state compared to the reactants. Understanding this important property is essential for understanding the shifts in molecular mobility and orientation that take place when reactants go from their initial state to the activated complex on the electrode surface. To calculate the entropy of activation, the Eyring equation (**Equation 1.30**), which is derived from transition state theory (TST) and is particularly useful in electrochemical processes, is typically utilized.

$$\Delta S^{0\neq} = 2.3R\,[\log j + \Delta H_{el}^{0\neq} / 2.3RT - \log (nF\omega C_{OH^-})] \quad \textbf{(1.30)}$$

Where, $\Delta S^{0\neq}$ is the standard entropy of activation,

j is the current density at overpotential,

n is the no. of electrons transferred, which is 4 e^- for the OER process,

ω is the frequency term (= k_BT/h),

C_{OH^-} is the hydroxide ion concentration,

k_B is the Boltzmann constant,

h is the Planck's constant.

An essential part of the OER process is the adsorption of intermediates like OH^-, O*, and OOH* onto the catalyst surface. The entropy shift that takes place during this process is determined by the interaction between the reactants and the electrode surface. When sticking to the electrode, the intermediates may adopt a more rigid orientation, reducing their degrees of freedom, as indicated by a negative entropy. This exemplifies strong adsorption processes, where the intermediates create a stable combination with the surface.

1.5.8. Stability

Stability is a crucial parameter for an efficient electrocatalyst in water splitting, alongside catalytic activity. To evaluate stability, two common electrochemical methods, chronoamperometry (CA) and chronopotentiometry (CP) are employed. Chronoamperometry involves monitoring the current variation over time at a fixed potential, while chronopotentiometry records potential variation over time at a fixed current density [71]. Additionally, CV at a high scan rate for over 1000 cycles, known as the accelerated degradation

test (ADT), is used to assess durability. A comparison of overpotential changes before and after linear sweep voltammetry (LSV) provides further insight into catalyst degradation. The ability of an electrocatalyst to retain its current density over extended periods reflects its long-term efficiency and suitability for large-scale or practical applications [72].

1.6. Objectives and Scope of the Thesis

This thesis focuses on developing cost-effective and efficient electrocatalysts for OER to advance renewable energy conversion technologies. Non-precious metal-based catalysts, particularly transition metal oxides (TMOs), were chosen for their high electrochemical activity, availability, and affordability. However, their poor conductivity and stability pose challenges for practical applications. To overcome these limitations, structural engineering and mixing with conducting polymers such as polypyrrole, strategies were employed to modify their electronic structure and enhance their catalytic performance.

The research aims to design electrocatalysts with a high active surface area, low overpotential, favorable Tafel slope, and improved durability, making them promising candidates for large-scale energy applications. The findings contribute to the ongoing development of efficient and sustainable materials for energy conversion technologies. In this context, we developed several multimetallic compounds and transition metal-based oxides, along with a composite incorporating a polymer. These materials were designed to enhance electrochemical performance by improving conductivity, stability, and catalytic activity for energy conversion reactions. The combination of multiple metal components and polymer-based composites aims to optimize structural and electronic properties, making them more

effective for practical applications in renewable energy technologies. Work performed in the present thesis can be summarized as follows-

1. The objective is to develop a low-cost, durable, and efficient material suitable for large-scale water oxidation applications. In this context, bismuth copper titanate (BCTO), with its perovskite structure, offers promising stability and catalytic properties, while magnesium doping is expected to enhance its electronic conductivity and active site density. This research aims to investigate the structural, electronic, and electrocatalytic changes induced by Mg doping in BCTO and to evaluate its performance as a robust OER catalyst.
2. Mixed metal oxides based on cobalt have demonstrated encouraging promise as effective and affordable electrocatalysts for the OER in alkaline media. Among them, cobalt tungstate ($Co_xW_{2-x}O_4$) provides a structure that may be adjusted, and the electrochemical performance can be greatly impacted by the Co/W ratio. The purpose of this study is to methodically examine how the material's structural, morphological, and catalytic characteristics are affected by different cobalt contents (x = 0.5, 1.0, and 1.5). To contribute to the development of high-performance non-noble metal electrocatalysts, the goal is to customize the composition to attain the best possible activity, stability, and kinetics for alkaline water oxidation.
3. Cobalt tungstate ($CoWO_4$) exhibits promising catalytic properties, while conductive polymers like polypyrrole (ppy) can enhance electron transport and stability. This study aims to synthesize and investigate a novel polypyrrole-integrated $CoWO_4$ composite to explore the synergistic effects between the metal oxide and polymer. The objective is to

improve catalytic performance by enhancing conductivity, active site accessibility, and long-term durability, paving the way for efficient, low-cost OER catalysts.

1.7. References

[1] J. Wu, Y. Huang, W. Ye, Y. Li, CO2 Reduction: From the Electrochemical to Photochemical Approach, Adv. Sci. 4 (2017). https://doi.org/10.1002/advs.201700194.

[2] M.G. Kibria, J.P. Edwards, C.M. Gabardo, C.T. Dinh, A. Seifitokaldani, D. Sinton, E.H. Sargent, Electrochemical CO2 Reduction into Chemical Feedstocks: From Mechanistic Electrocatalysis Models to System Design, Adv. Mater. 31 (2019). https://doi.org/10.1002/adma.201807166.

[3] F. Segura, J.A.- Resources, undefined 2015, Modular PEM fuel cell SCADA & simulator system, Mdpi.Com 4 (2015) 692–712. https://doi.org/10.3390/resources4030692.

[4] D.J. Torres, J. Crichigno, Influence of reflectivity and cloud cover on the optimal tilt angle of solar panels, Resources 4 (2015) 736–750. https://doi.org/10.3390/resources4040736.

[5] S.K. Jha, J. Bilalovic, A. Jha, N. Patel, H. Zhang, Renewable energy: Present research and future scope of Artificial Intelligence, Renew. Sustain. Energy Rev. 77 (2017) 297–317. https://doi.org/10.1016/j.rser.2017.04.018.

[6] M.D.- Resources, undefined 2015, Renewable energy development in small island developing states of the Pacific, Mdpi.ComM DornanResources, 2015•mdpi.Com 4 (2015) 490–506. https://doi.org/10.3390/resources4030490.

[7] M. Asif, T. Muneer, Energy supply, its demand and security issues for developed and emerging economies, Renew. Sustain. Energy Rev. 11 (2007) 1388–1413. https://doi.org/10.1016/j.rser.2005.12.004.

[8] S. Shafiee, E. Topal, When will fossil fuel reserves be diminished?, Energy Policy 37 (2009) 181–189. https://doi.org/10.1016/j.enpol.2008.08.016.

[9] M. Blondeel, M. Bradshaw, International oil companies, decarbonisation and transition risks, in: Handb. Oil Int. Relations, 2022: pp. 372–392. https://doi.org/10.4337/9781839107559.00034.

[10] R.B. Jackson, P. Friedlingstein, C. Le Quéré, S. Abernethy, R.M. Andrew, J.G. Canadell, P. Ciais, S.J. Davis, Z. Deng, Z. Liu, J.I. Korsbakken, G.P. Peters, Global fossil carbon emissions rebound near pre-COVID-19 levels, Environ. Res. Lett. 17 (2022) 031001. https://doi.org/10.1088/1748-9326/ac55b6.

[11] P.C.K. Vesborg, T.F. Jaramillo, Addressing the terawatt challenge: Scalability in the supply of chemical elements for renewable energy, RSC Adv. 2 (2012) 7933–7947. https://doi.org/10.1039/c2ra20839c.

[12] M. David, C. Ocampo-Martínez, R. Sánchez-Peña, Advances in alkaline water electrolyzers: A review, J. Energy Storage 23 (2019) 392–403.

https://doi.org/10.1016/j.est.2019.03.001.

[13] I.E.L. Stephens, J. Rossmeisl, I. Chorkendorff, Toward sustainable fuel cells, Science (80-.). 354 (2016) 1378–1379. https://doi.org/10.1126/science.aal3303.

[14] L. Dusonchet, S. Favuzza, F. Massaro, E. Telaretti, G. Zizzo, Technological and legislative status point of stationary energy storages in the EU, Renew. Sustain. Energy Rev. 101 (2019) 158–167. https://doi.org/10.1016/j.rser.2018.11.004.

[15] L. Li, Z. wen Chang, X.B. Zhang, Recent Progress on the Development of Metal-Air Batteries, Adv. Sustain. Syst. 1 (2017). https://doi.org/10.1002/adsu.201700036.

[16] X. Zhang, Z. Yang, Z. Lu, W. Wang, Bifunctional CoNx embedded graphene electrocatalysts for OER and ORR: A theoretical evaluation, Carbon N. Y. 130 (2018) 112–119. https://doi.org/10.1016/j.carbon.2017.12.121.

[17] Q. Zhang, H. Zhong, F. Meng, D. Bao, X. Zhang, X. Wei, Three-dimensional interconnected Ni(Fe)OxHy nanosheets on stainless steel mesh as a robust integrated oxygen evolution electrode, Nano Res. 11 (2018) 1294–1300. https://doi.org/10.1007/s12274-017-1743-8.

[18] Y.J. Wang, W. Long, L. Wang, R. Yuan, A. Ignaszak, B. Fang, D.P. Wilkinson, Unlocking the door to highly active ORR catalysts for PEMFC applications: Polyhedron-engineered Pt-based nanocrystals, Energy Environ. Sci. 11 (2018) 258–275. https://doi.org/10.1039/c7ee02444d.

[19] S. Shah, V. Venkatramanan, R. Prasad, Microbial fuel cell: Sustainable green technology for bioelectricity generation and wastewater treatment, in: Sustain. Green Technol. Environ. Manag., Springer Singapore, 2019: pp. 199–218. https://doi.org/10.1007/978-981-13-2772-8_10.

[20] Y. Zhao, B.P. Setzler, J. Wang, J. Nash, T. Wang, B. Xu, Y. Yan, An Efficient Direct Ammonia Fuel Cell for Affordable Carbon-Neutral Transportation, Joule 3 (2019) 2472–2484. https://doi.org/10.1016/j.joule.2019.07.005.

[21] D.E. Curtin, R.D. Lousenberg, T.J. Henry, P.C. Tangeman, M.E. Tisack, Advanced materials for improved PEMFC performance and life, J. Power Sources 131 (2004) 41–48. https://doi.org/10.1016/j.jpowsour.2004.01.023.

[22] R.M. Ormerod, Solid oxide fuel cells, Chem. Soc. Rev. 32 (2003) 17–28. https://doi.org/10.1039/b105764m.

[23] E. Gülzow, Alkaline fuel cells, in: Fuel Cells, John Wiley & Sons, Ltd, 2004: pp. 251–255. https://doi.org/10.1002/fuce.200400042.

[24] A.L. Dicks, Molten carbonate fuel cells, Curr. Opin. Solid State Mater. Sci. 8 (2004) 379–383. https://doi.org/10.1016/j.cossms.2004.12.005.

[25] A.S. Arico, V. Baglio, V. Antonucci, Direct methanol fuel cells, Johnson Matthey, 2010. https://doi.org/10.1595/003214096x404150159.

[26] Z.L. Wang, D. Xu, J.J. Xu, X.B. Zhang, Oxygen electrocatalysts in metal-air batteries: From aqueous to nonaqueous electrolytes, Chem. Soc. Rev. 43 (2014) 7746–7786. https://doi.org/10.1039/c3cs60248f.

[27] G. Nam, J. Cho, M. Liu, Recent Advances in Low-Cost, Highly Efficient Bi-Functional Oxygen Electrocatalysts for High-Performance Zinc-Air Batteries, ECS Meet. Abstr. MA2019-02 (2019) 50–50. https://doi.org/10.1149/ma2019-02/1/50.

[28] Y. Yan, B.Y. Xia, B. Zhao, X. Wang, A review on noble-metal-free bifunctional heterogeneous catalysts for overall electrochemical water splitting, J. Mater. Chem. A 4 (2016) 17587–17603. https://doi.org/10.1039/C6TA08075H.

[29] J.D. Blakemore, A. Gupta, J.J. Warren, B.S. Brunschwig, H.B. Gray, Noncovalent immobilization of electrocatalysts on carbon electrodes for fuel production, J. Am. Chem. Soc. 135 (2013) 18288–18291. https://doi.org/10.1021/ja4099609.

[30] E. Fabbri, T.J. Schmidt, Oxygen Evolution Reaction - The Enigma in Water Electrolysis, ACS Catal. 8 (2018) 9765–9774. https://doi.org/10.1021/acscatal.8b02712.

[31] F.M. Sapountzi, J.M. Gracia, C.J. (Kee. J. Weststrate, H.O.A. Fredriksson, J.W. (Hans. Niemantsverdriet, Electrocatalysts for the generation of hydrogen, oxygen and synthesis gas, Prog. Energy Combust. Sci. 58 (2017) 1–35. https://doi.org/10.1016/j.pecs.2016.09.001.

[32] M. Tahir, L. Pan, F. Idrees, X. Zhang, L. Wang, J.J. Zou, Z.L. Wang, Electrocatalytic oxygen evolution reaction for energy conversion and storage: A comprehensive review, Nano Energy 37 (2017) 136–157. https://doi.org/10.1016/j.nanoen.2017.05.022.

[33] T. Reier, M. Oezaslan, P. Strasser, Electrocatalytic oxygen evolution reaction (OER) on Ru, Ir, and pt catalysts: A comparative study of nanoparticles and bulk materials, ACS Catal. 2 (2012) 1765–1772. https://doi.org/10.1021/cs3003098.

[34] Y. Lee, J. Suntivich, K.J. May, E.E. Perry, Y. Shao-Horn, Synthesis and activities of rutile IrO 2 and RuO 2 nanoparticles for oxygen evolution in acid and alkaline solutions, J. Phys. Chem. Lett. 3 (2012) 399–404. https://doi.org/10.1021/JZ2016507/SUPPL_FILE/JZ2016507_SI_001.PDF.

[35] A. Soni, S.K. Maurya, M. Malviya, Exploring electrocatalysts for oxygen evolution: A comprehensive comparative review in alkaline and acidic medium, J. Power Sources 636 (2025). https://doi.org/10.1016/j.jpowsour.2025.236571.

[36] Z. Feng, C. Dai, P. Shi, X. Lei, R. Guo, B. Wang, X. Liu, J. You, Seven mechanisms of oxygen evolution reaction proposed recently: A mini review, Chem. Eng. J. 485 (2024). https://doi.org/10.1016/j.cej.2024.149992.

[37] X. Ren, Y. Zhai, N. Yang, B. Wang, S. Liu, Lattice Oxygen Redox Mechanisms in the Alkaline Oxygen Evolution Reaction, Adv. Funct. Mater. 34 (2024).

https://doi.org/10.1002/adfm.202401610.

[38] S. Hao, M. Liu, J. Pan, X. Liu, X. Tan, N. Xu, Y. He, L. Lei, X. Zhang, Dopants fixation of Ruthenium for boosting acidic oxygen evolution stability and activity, Nat. Commun. 11 (2020). https://doi.org/10.1038/s41467-020-19212-y.

[39] M. Kodera, Y. Kawahara, Y. Hitomi, T. Nomura, T. Ogura, Y. Kobayashi, Reversible O-O bond scission of peroxodiiron(III) to high-spin oxodiiron(IV) in dioxygen activation of a diiron center with a bis-tpa dinucleating ligand as a soluble methane monooxygenase model, J. Am. Chem. Soc. 134 (2012) 13236–13239. https://doi.org/10.1021/ja306089q.

[40] C. Rong, K. Dastafkan, Y. Wang, C. Zhao, Breaking the Activity and Stability Bottlenecks of Electrocatalysts for Oxygen Evolution Reactions in Acids, Adv. Mater. 35 (2023) 2211884. https://doi.org/10.1002/adma.202211884.

[41] P.K. Shen, C.-Y. Wang, S.P. Jiang, X. Sun, J. Zhang, Electrochemical energy : advanced materials and technologies, in: Electrochem. Energy Storage Convers., CRC Press, 2016. https://doi.org/10.1201/9781351228756/ELECTROCHEMICAL-ENERGY-PEI-KANG-SHEN-CHAO-YANG-WANG-SAN-PING-JIANG-XUELIANG-SUN-JIUJUN-ZHANG.

[42] L. Han, S. Dong, E. Wang, Transition-Metal (Co, Ni, and Fe)-Based Electrocatalysts for the Water Oxidation Reaction, Adv. Mater. 28 (2016) 9266–9291. https://doi.org/10.1002/adma.201602270.

[43] X. Gong, A. Li, J. Wu, J. Wang, C. Wang, J. Wang, Graphene-cobalt based oxygen electrocatalysts, Catal. Today 358 (2020) 184–195. https://doi.org/10.1016/j.cattod.2019.10.027.

[44] B.E. Conway, M. Salomon, Electrochemical reaction orders: Applications to the hydrogen- and oxygen-evolution reactions, Electrochim. Acta 9 (1964) 1599–1615. https://doi.org/10.1016/0013-4686(64)80088-8.

[45] J. MacDonald, B.C.-P. of The, U. 1962, The role of surface films in the kinetics of oxygen evolution at Pd + Au alloy electrodes, Proc. R. Soc. London. Ser. A. Math. Phys. Sci. 269 (1962) 419–440. https://doi.org/10.1098/rspa.1962.0186.

[46] G. Zhang, Y. Li, X. Xiao, Y. Shan, Y. Bai, H.G. Xue, H. Pang, Z. Tian, Q. Xu, In Situ Anchoring Polymetallic Phosphide Nanoparticles within Porous Prussian Blue Analogue Nanocages for Boosting Oxygen Evolution Catalysis, Nano Lett. 21 (2021) 3016–3025. https://doi.org/10.1021/acs.nanolett.1c00179.

[47] J.S. Yoo, X. Rong, Y. Liu, A.M. Kolpak, Role of Lattice Oxygen Participation in Understanding Trends in the Oxygen Evolution Reaction on Perovskites, ACS Catal. 8 (2018) 4628–4636. https://doi.org/10.1021/acscatal.8b00612.

[48] Z. Chen, C.X. Kronawitter, X. Yang, Y.W. Yeh, N. Yao, B.E. Koel, The promoting effect of tetravalent cerium on the oxygen evolution activity of copper oxide catalysts,

Phys. Chem. Chem. Phys. 19 (2017) 31545–31552. https://doi.org/10.1039/c7cp05248k.

[49] S.C. Chou, K.C. Tso, Y.C. Hsieh, B.Y. Sun, J.F. Lee, P.W. Wu, Facile synthesis of Co3O4@CoO@Co gradient core@shell nanoparticles and their applications for oxygen evolution and reduction in alkaline electrolytes, Materials (Basel). 13 (2020) 1–14. https://doi.org/10.3390/ma13122703.

[50] A. Karmakar, S.K. Srivastava, Transition-Metal-Substituted Cobalt Carbonate Hydroxide Nanostructures as Electrocatalysts in Alkaline Oxygen Evolution Reaction, ACS Appl. Energy Mater. 3 (2020) 7335–7344. https://doi.org/10.1021/acsaem.0c00623.

[51] S. Zhang, B. Huang, L. Wang, X. Zhang, H. Zhu, X. Zhu, J. Li, S. Guo, E. Wang, Boosted Oxygen Evolution Reactivity via Atomic Iron Doping in Cobalt Carbonate Hydroxide Hydrate, ACS Appl. Mater. Interfaces 12 (2020) 40220–40228. https://doi.org/10.1021/acsami.0c07260.

[52] V.S. Rai, S. Pandey, V. Kumar, M.K. Verma, A. Kumar, S. Singh, D. Prajapati, K.D. Mandal, Investigation of microstructure and dielectric behavior of Bi2/3Cu3−xMgxTi4O12 (x = 0, 0.05, 0.1 and 0.2) ceramics synthesized by semi-wet route, J. Mater. Sci. Mater. Electron. 32 (2021) 7671–7680. https://doi.org/10.1007/s10854-021-05483-8.

[53] S. Kumar Maurya, A. Soni, M. Malviya, D. Tiwary, Understanding the electrocatalytic role of magnesium doped bismuth copper titanate (BCTO) in oxygen evolution reaction, J. Electroanal. Chem. 975 (2024) 118803. https://doi.org/10.1016/j.jelechem.2024.118803.

[54] X. Ji, M. Ma, R. Ge, X. Ren, H. Wang, J. Liu, Z. Liu, A.M. Asiri, X. Sun, WO3 Nanoarray: An Efficient Electrochemical Oxygen Evolution Catalyst Electrode Operating in Alkaline Solution, Inorg. Chem. 56 (2017) 14743–14746. https://doi.org/10.1021/acs.inorgchem.7b02552.

[55] L.N. Nguyen, U.T.D. Thuy, Q.D. Truong, I. Honma, Q.L. Nguyen, P.D. Tran, Electrodeposited Amorphous Tungsten-doped Cobalt Oxide as an Efficient Catalyst for the Oxygen Evolution Reaction, Chem. - An Asian J. 13 (2018) 1530–1534. https://doi.org/10.1002/asia.201800401.

[56] F. Wei, Q. Peng, T. Sun, J. Zhu, Z. Luo, D. Wang, X. Yang, S. Sun, B. Wu, Reversible Oxygen Vacancies in Tungsten Oxide-Activated Heterocatalysts Enable Stable Electrocatalytic Oxygen Evolution, Nano Energy (2025) 110961. https://doi.org/10.1016/j.nanoen.2025.110961.

[57] P.A. Shinde, S.C. Jun, Review on Recent Progress in the Development of Tungsten Oxide Based Electrodes for Electrochemical Energy Storage, ChemSusChem 13 (2020) 11–38. https://doi.org/10.1002/cssc.201902071.

[58] S.R. Bhosale, R.R. Bhosale, D.N. Patil, R.P. Dhavale, G.B. Kolekar, V.B. Shimpale, P.

V. Anbhule, Bioderived Mesoporous Carbon@Tungsten Oxide Nanocomposite as a Drug Carrier Vehicle of Doxorubicin for Potent Cancer Therapy, Langmuir 39 (2023) 11910–11924. https://doi.org/10.1021/acs.langmuir.3c01715.

[59] W. Sun, C. Li, J. Bai, L. Xing, Carbon Nanofibers-Assembled Tungsten Oxide as Unique Hybrid Electrode Materials for High-Performance Symmetric Supercapacitors, Energy and Fuels 35 (2021) 11572–11579. https://doi.org/10.1021/acs.energyfuels.1c01428.

[60] N.H. Alotaibi, S. Manzoor, S. Saleem, S. Mohammad, M. Khalil, Ş. Yalçin, A.G. Abid, S.I. Allakhverdiev, Rational development of PPy/CuWO4 nanostructure as competent electrocatalyst for oxygen evolution, and hydrogen evolution reactions, Int. J. Hydrogen Energy 59 (2024) 1326–1334. https://doi.org/10.1016/j.ijhydene.2024.02.125.

[61] L. Fan, J. Sunarso, X. Zhang, X. Xiong, L. He, L. Luo, F. Wang, Z. Fan, C. Wu, D. Han, N.H. Wong, Y. Wang, G. Chen, W. Chen, Regulating the hole transfer from CuWO4 photoanode to NiWO4 electrocatalyst for enhanced water oxidation performance, Int. J. Hydrogen Energy 47 (2022) 20153–20165. https://doi.org/10.1016/j.ijhydene.2022.04.148.

[62] A.M. El Sayed, M.I.A. Abdel Maksoud, S.M. Kassem, A.S. Awed, Synthesis, structural, optical, and dielectric properties of CuWO4/PVP/Cs bio-nanocomposites for some industrial applications, J. Mater. Sci. Mater. Electron. 34 (2023). https://doi.org/10.1007/s10854-023-11118-x.

[63] K. Brijesh, K. Bindu, D. Shanbhag, H.S. Nagaraja, Chemically prepared Polypyrrole/ZnWO 4 nanocomposite electrodes for electrocatalytic water splitting, Int. J. Hydrogen Energy 44 (2019) 757–767. https://doi.org/10.1016/j.ijhydene.2018.11.022.

[64] R. Ansari, Polypyrrole Conducting Electroactive Polymers: Synthesis and Stability Studies, J. Chem. 3 (2006) 186–201. https://doi.org/10.1155/2006/860413.

[65] A. Soni, S. Kumar Maurya, M. Malviya, D. Tiwary, Exploring the synergistically enhanced activity of novel α-MnSe/ppy composite for superior OER catalyst in alkaline medium, J. Electroanal. Chem. 972 (2024) 118640. https://doi.org/10.1016/j.jelechem.2024.118640.

[66] A. Soni, S.K. Maurya, M. Malviya, B. Lal, D. Tiwary, Evaluating Zn ferrite (ZnxFe3-xO4; $0 \leq x \leq 1$) for alkaline water oxidation: electrochemical and spectro-electrochemical study, J. Appl. Electrochem. 55 (2024) 147–161. https://doi.org/10.1007/s10800-024-02164-2.

[67] S. Anantharaj, S.R. Ede, K. Karthick, S. Sam Sankar, K. Sangeetha, P.E. Karthik, S. Kundu, Precision and correctness in the evaluation of electrocatalytic water splitting: Revisiting activity parameters with a critical assessment, Energy Environ. Sci. 11 (2018) 744–771. https://doi.org/10.1039/c7ee03457a.

[68] Q. Zhao, C. Meng, D. Kong, Y. Wang, H. Hu, X. Chen, Y. Han, X. Chen, Y. Zhou, M. Lin, M. Wu, In Situ Construction of Nickel Sulfide Nano-Heterostructures for Highly Efficient Overall Urea Electrolysis, ACS Sustain. Chem. Eng. 9 (2021) 15582–15590. https://doi.org/10.1021/acssuschemeng.1c05722.

[69] I. Herraiz-Cardona, E. Ortega, J.G. Antón, V. Pérez-Herranz, Assessment of the roughness factor effect and the intrinsic catalytic activity for hydrogen evolution reaction on Ni-based electrodeposits, Int. J. Hydrogen Energy 36 (2011) 9428–9438. https://doi.org/10.1016/j.ijhydene.2011.05.047.

[70] A.S. Chaddha, N.K. Singh, M. Malviya, A. Sharma, Birnessite-clay mineral couple in the rock varnish: a nature's electrocatalyst, Sustain. Energy Fuels 6 (2022) 2553–2569. https://doi.org/10.1039/d2se00185c.

[71] N.T. Suen, S.F. Hung, Q. Quan, N. Zhang, Y.J. Xu, H.M. Chen, Electrocatalysis for the oxygen evolution reaction: Recent development and future perspectives, Chem. Soc. Rev. 46 (2017) 337–365. https://doi.org/10.1039/c6cs00328a.

[72] C. Yang, Y. Lu, W. Duan, Z. Kong, Z. Huang, T. Yang, Y. Zou, R. Chen, S. Wang, Recent Progress and Prospective of Nickel Selenide-Based Electrocatalysts for Water Splitting, Energy and Fuels 35 (2021) 14283–14303. https://doi.org/10.1021/acs.energyfuels.1c01854.